Supporting Information

Conte et al. 10.1073/pnas.0914785107

SI Materials and Methods

Controls for Mo Injections. The blocking efficiencies of Mo-miR-204-1 and Mo-miR-204-2 were verified using two different mRNA reporter approaches (Fig. S1 *C–L*). The first was a "direct assay," which measured Mo interference with the translation of a reporter. The reporter was the 5′-UTR of the EGFP coding sequence fused to the stretch of ol-miR-204- and ol-miR-204-2 sequences complementary to those of the selected Mo (Fig. S1*C*). Injections of both Mo-miR-204-1 and Mo-miR-204-2 specifically abolished the EGFP signal (Fig. S1 *D–G*). In the second "blocking approach," the selected Mo was tested for its efficiency of inhibition of the processing of miR-204 precursor sequences, which were inserted in the 3′-UTR of a destabilized d1-EGFP (Fig. S1*H*). Both Mos blocked maturation of the miR-204, maintaining the integrity of the 3′-UTR and the stability of the mRNA, and thus the expression of the d1-EGFP protein (Fig. S1 *I–L*). Control mm-Mo-miR-204 had no significant effects in these assays and did not affect endogenous miR-204 expression. Injections of both Mo-miR-204-1 and Mo-miR-204-2 resulted in significant down-regulation of miR-204 levels, as shown by RNA ISH (Fig. S1 *A* and *B*).

The efficacy of Meis2-TPmiR-204 Mo was tested using the direct assay (described above) and a "protection approach," which measured the Mo interference with *Meis2* targeting by miR-204. In the latter approach, the reporter was the 3′-UTR of *olMeis2,* which was inserted downstream of the destabilized d1-EGFP reporter gene (Fig. S3*A*). Meis2-TPmiR-204 Mo injections protected the miR-204 target site of the d1-EGFP-*olMeis2*-3′-UTR reporter gene from miR-204 duplex binding (Fig. S3 *B–E*). The inhibitory efficiency of this Mo was measured by quantifying EGFP intensity, as reported previously (1), and with ImageJ (National Institutes of Health) analysis. Possible nonspecific effects of Meis2-TPmiR-204 were ruled out by coinjecting it with a Mo designed against p53, a key protein in the apoptotic pathway. Indeed, activation of p53 is an occasional off-targeting effect of Mo injections (2), which can be counteracted by injection of a p53 Mo. Consistent with the specificity of the Meis2-TPmiR-204–induced eye phenotype, both miR-204 and Mo-Meis2 injections were sufficient to rescue the lens and coloboma phenotypes (Fig. S2 *P–U* and Table S2).

1. Esteve P, Lopez-Rios J, Bovolenta P (2004) SFRP1 is required for the proper establishment of the eye field in the medaka fish. *Mech Dev* 121:687–701.

2. Robu ME, et al. (2007) p53 activation by knockdown technologies. *PLoS Genet* 3:e78.

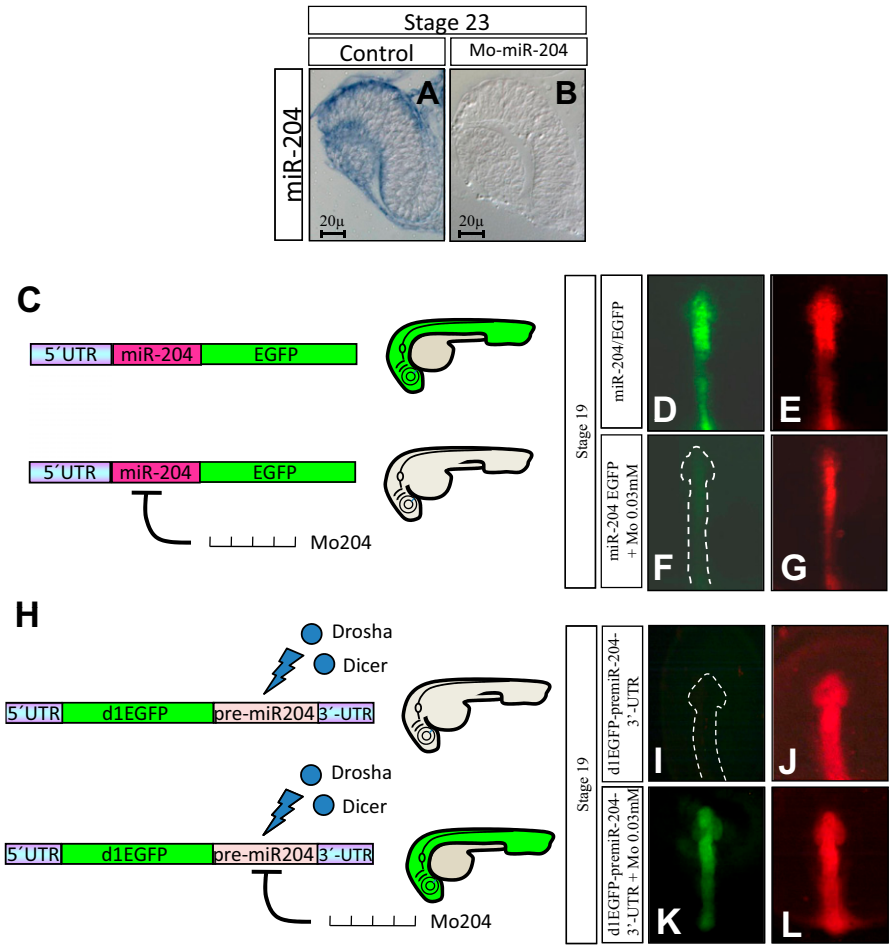

Fig. S1. Mo-miR-204 specifically blocks miR-204 maturation and processing. Frontal vibratome sections from control (*A*) and Mo-miR-204–injected (*B*) embryos hybridized with a digoxigenin-labeled miR-204–specific probe. (*B*) miR-204 expression was not detected in morphants. (*C*) Schematic representation of the direct assay used to assess efficiency of the two Mos designed to block the miR-204 mature sequence (*SI Text*). (*D*–*G*) Representative embryos injected with the synthetic mRNAs encoding the reporter construct alone (*D* and *E*) or together with Mo-miR-204 (*F* and *G*). Note that 0.03 mM Mo-miR-204 was sufficient to abolish EGFP reporter expression completely. (*H*) Schematic representation of the blocking approach used to test Mo ability to interfere with maturation of miR-204 precursor sequences (*SI Text*). (*I*–*L*) Representative embryos injected with the synthetic mRNAs encoding the reporter construct alone (*I* and *J*) or together with Mo-miR-204 (*K* and *L*). Maturation of miR-204 precursors is abolished by Mo-miR-204, allowing d1-EGFP expression (*I* and *K*) (*SI Text*). Red fluorescent protein serves as an injection control.

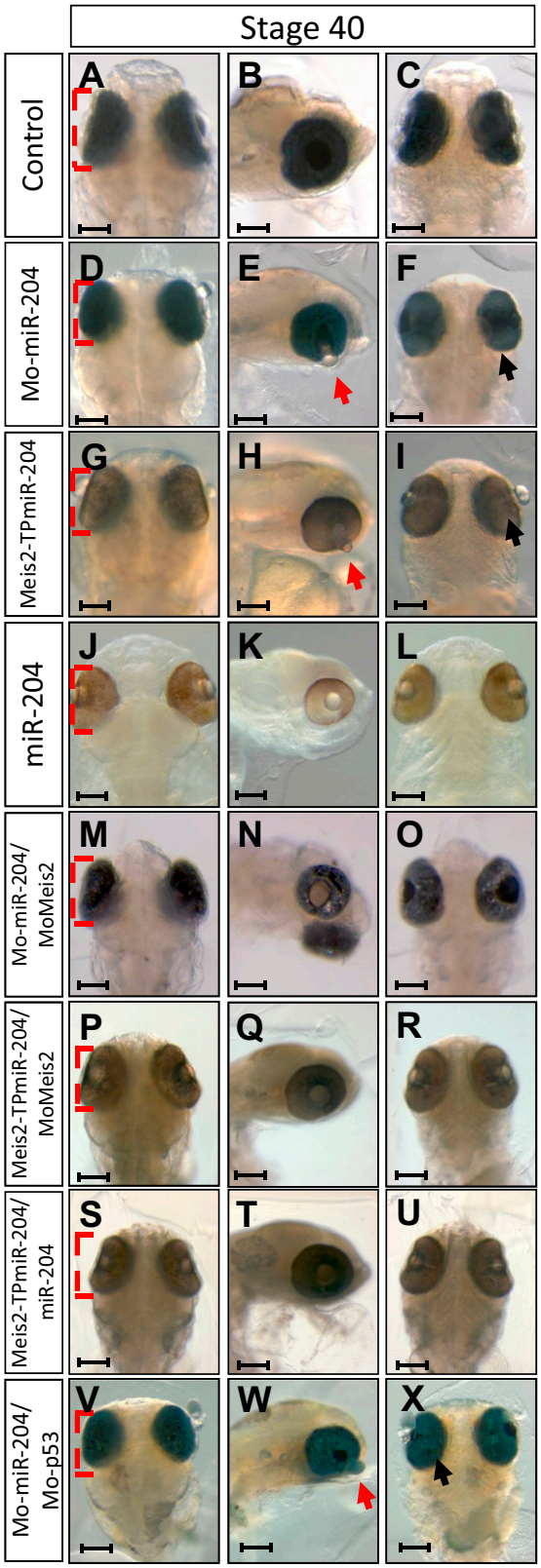

Fig. S2. Alterations in levels of miR-204 result in defects in medaka eye development. Bright-field stereomicroscopy images of control (*A*–*C*), Mo-miR-204 (*D*–*F*), Meis2-TPmiR-204 (*G*–*I*), miR-204 (*J*–*L*), Mo-miR-204/MoMeis2 (*M*–*O*), Meis2-TPmiR-204/MoMeis2 (*P*–*R*), Meis2-TPmiR-204/miR-204 (*S*–*U*), and Mo-miR-204/Mo-p53 (*V*–*X*) –injected medaka embryos as dorsal (*A*, *D*, *G*, *J*, *M*, *P*, *S*, and *V*), lateral (*B*, *E*, *H*, *K*, *N*, *Q*, *T*, and *W*), and ventral (*C*, *F*, *I*, *L*, *O*, *R*, *U*, and *X*) views. All treated embryos are microphthalmic (*D*, *G*, *J*, *M*, *P*, *S*, and *V*, red broken line) when compared with controls (*A*). (*B*, *E*, *H*, and *W*) In Mo-miR-204, Meis2-TPmiR-204, and Mo-miR-204/Mo-p53–injected embryos, the lens protrudes out of the optic cup (*E*, *H*, and *W*, red arrows), which also shows fissure coloboma (*F*, *I*, and *X*, black arrows). Embryos shown in *J*–*L* were treated with 1-phenyl-2-thiourea to reduce pigmentation. (Scale bars: 50 μm.)

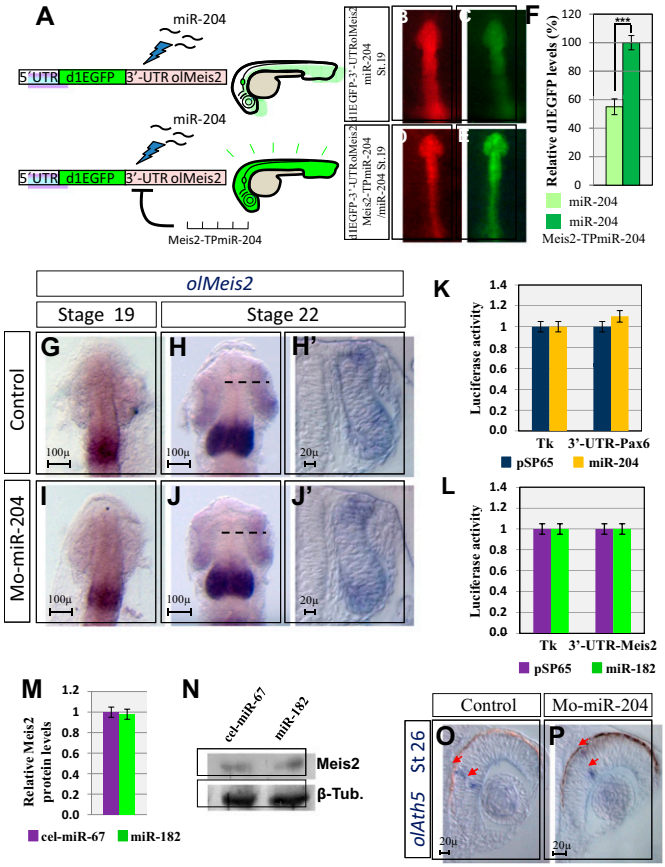

Fig. S3. *Meis2* is a specific miR-204 target. (*A*) Schematic representation of the protector assay to assess efficiency of the Meis2-TPmiR-204-Mo designed to block binding of miR-204 to its predicted target site in *Meis2* 3′-UTR (*SI Text*). (*B*–*E*) Representative embryos coinjected with the synthetic mRNA encoding the reporter d1GFP-3′-UTR-olMeis2 construct and the mir-204 duplexes (*B* and *C*) or with miR-204 and Meis2-TPmiR-204 (*D* and *E*). (*F*) Efficiency of Meis2-TPmiR-204 inhibition of d1GFP repression when Mo and miR-204 mimic are coinjected in embryos at the one/two-cell stage (*SI Text*). ***$P < 0.0001$ (*t* tests). Red fluorescent protein serves as a control for the injection and is also used to normalize GFP fluorescence. Control (*G*–*H*′) and Mo-miR-204–injected (*I* and *J*′) embryos are hybridized in whole-mount RNA ISH with the *olMeis2* probe at St19 and St22 (as indicated). Note that morphology of the eye and levels of *olMeis2* expression in the lens placode and neuroretina are normal (*H*′ and *J*′). (*K*–*L*) Relative Luc activities in H36CE cells are presented as fold differences in the Luc/Renilla ratios normalized to the Luc reporter constructs. Addition of miR-204 or miR-182 did not significantly decrease the Luc activity of the constructs containing the 3′UTR of *PAX6* (*K*) or *MEIS2* (*L*). Densitometric analysis (*M*) of Western blotting (N) shows that in H36CE cells, Meis2 protein levels are unaltered in the presence of miR-182 duplexes when compared with cel-miR-67 control transfections. Relative levels of the Meis2 protein measured 48 h after transfection of H36CE cells. Frontal sections of St24 control (*O*) and Mo-miR-204 (*P*)–injected embryos hybridized in whole-mount RNA ISH with the *olAth5* probe. Note that the early retinal ganglion cell marker *Ath5* was correctly expressed in miR-204 morphants at St26 (red arrows). (Scale bars: *G*, *H*, *I*, and *J*, 100 μm; *H*′, *J*′, *O*, and *P*, 20 μm.)

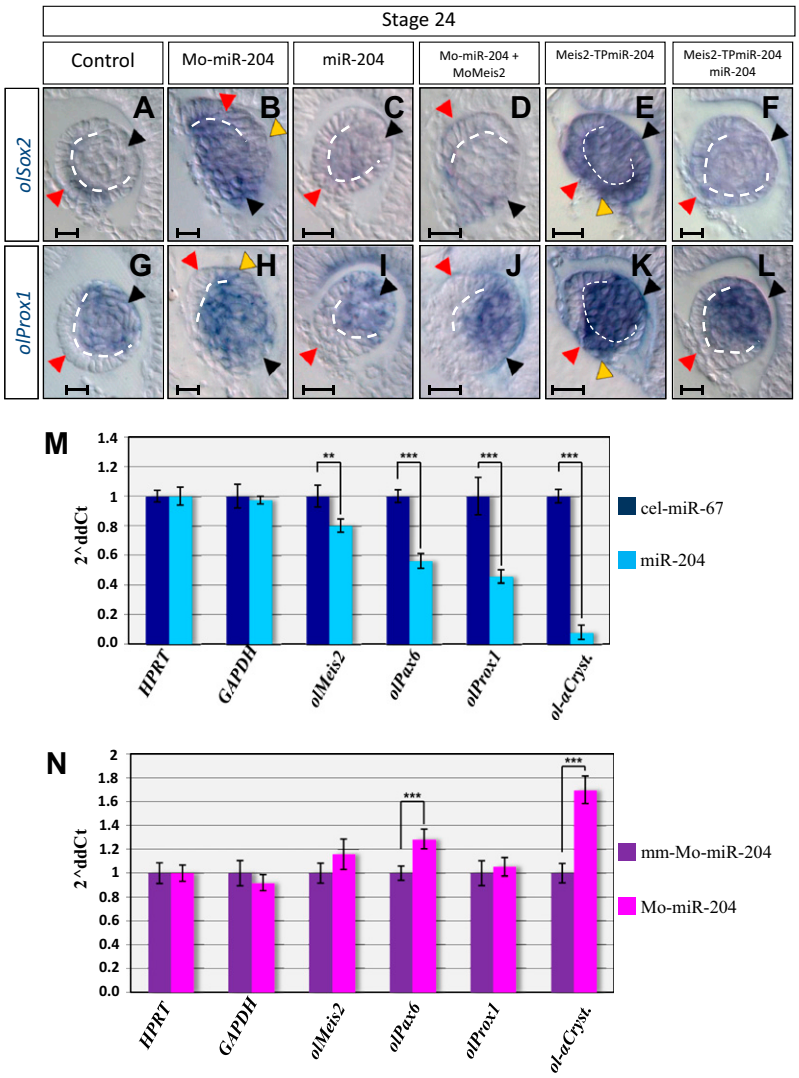

Fig. S4. Interference with miR-204 affects the lens differentiation pathway via *Meis2* targeting. Frontal sections of St24 control (*A* and *G*), Mo-miR-204 (*B* and *H*), miR-204–overexpressing (*C* and *I*), Mo-Meis2/Mo-miR-204 (*D* and *J*), Meis2-TPmiR-204 (*E* and *K*), and Meis2-TPmiR-204/miR-204 (*F* and *L*)–injected medaka embryos hybridized in whole-mount RNA ISH with probes for *olSox2* (*A*–*F*) and *olProx1* (*G*–*L*). Expression levels of *olSox2* (*B* and *E*) and *olProx1* (*H* and *K*) are increased in lens placode and expanded into the epithelial lens monolayer of the morphants (*B*, *H*, *E*, and *K*, yellow arrowheads). The lens epithelial (*B* and *H*, red arrowheads) and primary fiber (*B* and *H*, black arrowheads) cells are mislocalized. miR-204 gain-of-function causes opposite effects in lens gene expression, but the lens epithelial monolayer (red arrowheads) and primary fibers (black arrowheads) are positioned normally (*C* and *I*). Mo-Meis2/Mo-miR-204 and Meis2-TPmiR-204/miR-204 coinjections restore correct expression of lens differentiation markers (*D*, *J*, *F*, and *L*), but Mo-Meis2/Mo-miR-204 injections do not rescue cell position (*D* and *J*, red and black arrowheads). Broken lines mark the epithelial monolayer/primary fiber boundary. (Scale bars: 20 μm.) (*M* and *N*) Fold changes (expressed as $2^{-\Delta\Delta Ct}$ values) in mRNA levels of *HPRT*, *GAPDH*, *olMeis2*, *olPax6*, *olProx1*, and olα-*ACrystallin* quantified by qRT-PCR from miR-204 compared with cel-miR-67 (*M*) and Mo-miR-204 compared with mm-Mo-miR204 (*N*)–injected embryos. $^{**}P < 0.001$; $^{***}P < 0.0001$ (*t* tests).

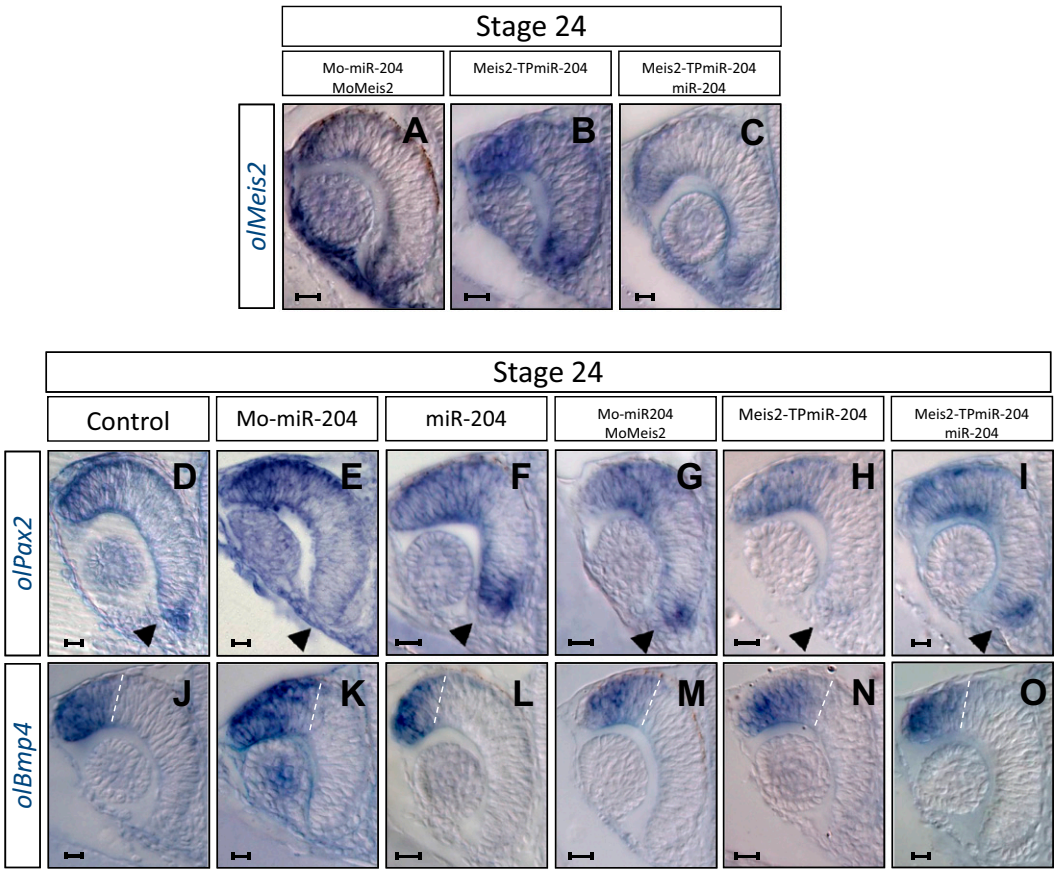

Fig. S5. miR-204 is required for maintenance of D-V eye polarity. Frontal sections of St24 Mo-Meis2/Mo-miR-204 (*A*), Meis2-TPmiR-204 (*B*), and Meis2-TPmiR-204/miR-204 (*C*) –injected embryos hybridized in whole-mount RNA ISH with the *olMeis2* probe. Compare *A*–*C* with Fig. 1 *H*–*J*. Expression of *olMeis2* (*B*) is up-regulated in the retina of Meis2-TPmiR-204 morphant embryos. Meis2-TPmiR-204/miR-204 coinjections restore correct expression of *olMeis2*. (*D*–*O*) Control (*D* and *J*), Mo-miR-204 (*E* and *K*), miR-204 (*F* and *L*), Mo-Meis2/Mo-miR-204 (*G* and *M*), Meis2-TPmiR-204 (*H* and *N*), and Meis2-TPmiR-204/miR-204 (*I* and *O*)–injected embryos hybridized in whole-mount RNA ISH with probes specific for *olPax2* (*D*–*I*) and *olBmp4* (*J*–*O*). Expression of ventral *olPax2* gene is absent, whereas that of dorsal marker *olBmp4* is expanded ventrally in morphants (*E*, *K*, *H*, and *N*) when compared with control embryos (*D* and *J*). miR-204–overexpressing embryos show the opposite pattern of D-V marker expression (*F* and *L*). Alterations in D-V polarity are rescued by Mo-miR-204/Mo-Meis2 (*G* and *M*) and Meis2-TPmiR-204/miR-204 (*I* and *O*) coinjections. Arrowheads illustrate the ventral *olPax2* expression domain in the retina. Broken lines illustrate the ventral-most boundary of *olBmp4* expression domain in the retina. (Scale bars: 20 μm.)

Table S1. Sequences of Mos and oligonucleotides used to generate constructs and RNA ISH templates or to carry out qRT-PCR

Name	Sequence	Concentration used, mM
Mos		
Mo-olmiR-204-1	5′-TTGATTCCAGGCATAGGATGACAAAGGGAAG-3′	0.09
Mo-olmiR-204-2	5′-CAAGCTCCAGGCATAGGATGACAAAGGGAAG-3′	0.09
mmMo-olmiR-204	5′-TTCATTGCAGCCATAGCATGAGAAAGCGAAG-3′	0.09
Mo-olp53	5′-CGGGAATCGCACCGACAACAATACG-3′	0.09
Mo-olMeis2	5′-GCGCTCCAATAAACTCCCGAATATG-3′	0.03
Meis2-TPmiR-204	5′- CCTGTTGTGGTAACAAAGTTCCCTT-3′	0.09
Oligonucleotide primers		
Control-Mo204/F	GATCCCTTCCCTTTGTCATCCTATGCCTGGAATCAAGCC	
Control-Mo204/R	CATGGGCTTGATTCCAGGCATAGGATGACAAAGGGAAGG	
Pax6-3′-UTR-SpeI/F	GACTAGTTTGTGTTAATTCAGTCAGTGAC	
Pax6-3′-UTR-SpeI/R	GACTAGTAAATACAAAGGCTTTGGCATG	
Meis2-3′-UTR-XbaI/F	GCTCTAGATATAAGGGAACTCAAGGGAA	
Meis2-3′-UTR-XbaI/R	GCTCAGACATAACGTCACAGTCCTCAT	
olMeis2-3′-UTR-XbaI/F	TGCACTGCAGTGCAAGTACTGGAGGACAAGGCAT	
olMeis2-3′-UTR-XbaI/R	TGCACTGCAGTGCAGAATCTTCTGGAGAGATCCG	
hsa-premiR-204-BglII/F	GAAGATCTCAGGGTGATGGAAAGGAGG	
hsa-premiR-204-XhoI/R	CCGCTCGAGCATGTCATGGAAATCCCAATGC	
hsa-premiR-182/F	gaagatctcatcctaactgtctctgtct	
hsa-premiR-182/R	ccgctcgagtcctcgcggagaacagcagg	
ol-premiR-204-1-PstI/F	AAAACTGCAGGGTGTTCAGTATTGCTTCTAG	
ol-premiR-204-1-NsiI/R	TGCATGCATTTAAAGATGACGACACGTGC	
ol-premiR-204-2-PstI/F	AACTGCAGGGAGAAGCATATCTCTCTGCA	
ol-premiR-204-2-NsiI/R	TGCATGCATCCGAGCAGTTTGTAACCATGT	
ACRYSTALLIN forward	CGTGAAGGTGATCGATGACT	
ACRYSTALLIN reverse	AGCAGTCCATCGGCAGACA	
Prox1 forward	ATCTCACCTTACTCAGGCAG	
Prox1 reverse	TAAGCATGTTGGAGCTTGGG	
Meis2 forward	AGTACTGGAGGACAAGGCAT	
Meis2 reverse	AAATAGGATTTGTCAGGCTGC	
Pax6 forward	GGGAGAAAACACCAACTCCA	
Pax6 reverse	ACATCCGGGTAATGGGTTCT	
Hprt forward	CTGAACAGGAACAGCGACC	
Hprt reverse	TGAGGAGCTCCAATAACGTC	
Gapdh forward	CGGCAAGCTGATAGTCGATG	
Gapdh reverse	AGAAACACTCCGGTGGACTC	

Table S2. Concentrations and frequencies of phenotypes observed after single or combined injections of Mo, mimic miR-204, and miRNA

		Frequency of morphological eye phenotype (% ± SD) of *n*					Frequency of molecular eye phenotype (% ± SD) of *n*	
Name (*n*)	Concentration, μM	Microphthalmia	Lens herniation	Lens epithelial-cell malposition	Coloboma	Toxicity (% ± SD) of *n*	Alteration in expression pattern of lens markers	Alteration in expression pattern of retinal D-V markers
Mo-olmiR-204-1 (256)	30	25 ± 5	23 ± 3	23 ± 3	8 ± 1	0 ± 1	NA	NA
Mo-olmiR-204-1 (288)	60	50 ± 5	45 ± 4	45 ± 4	15 ± 2	1 ± 2	NA	NA
Mo-olmiR-204-1 (3,000)	90	65 ± 5	59 ± 5	59 ± 5	22 ± 3	2 ± 2	59 ± 5	22 ± 3
Mo-olmiR-204-1 (322)	120	67 ± 5	61 ± 5	61 ± 5	23 ± 2	3 ± 2	NA	NA
Mo-olmiR-204-1/ Mo-olp53 (222)	90/90	65 ± 5	59 ± 5	59 ± 5	22 ± 3	2 ± 2	NA	NA
Mo-olmiR-204-1/Mo-olMeis2 (1,500)	90/30	42 ± 5	5 ± 2	42 ± 5	1 ± 1	2 ± 3	3 ± 2	1 ± 1
mmMo-olmiR-204 (2,560)	30–120	0 ± 0	0 ± 0	0 ± 0	0 ± 0	2 ± 1	0 ± 0	0 ± 0
Meis2-TPmiR-204 (158)	30	12 ± 5	10 ± 4	0 ± 0	4 ± 1	0 ± 1	NA	NA
Meis2-TPmiR-204 (267)	60	28 ± 5	25 ± 4	0 ± 0	9 ± 2	1 ± 2	NA	NA
Meis2-TPmiR-204 (1,250)	90	45 ± 5	40 ± 5	0 ± 0	12 ± 2	2 ± 1	40 ± 5	12 ± 2
Meis2-TPmiR-204 (232)	120	46 ± 5	41 ± 5	0 ± 0	15 ± 4	3 ± 1	NA	NA
Meis2-TPmiR-204/Mo-olp53 (272)	90/90	46 ± 5	40 ± 5	0 ± 0	12 ± 2	2 ± 1	NA	NA
Meis2-TPmiR-204/ miR-204 (1,500)	90/3	13 ± 4	2 ± 1	0 ± 0	1 ± 1	2 ± 1	3 ± 1	1 ± 1
Meis2-TPmiR-204/ Mo-olMeis2 (1,500)	90/30	33 ± 5	2 ± 1	0 ± 0	1 ± 1	2 ± 1	2 ± 1	1 ± 1
Mo-olMeis2 (380)	30	30 ± 2	0 ± 0	0 ± 0	0 ± 0	2 ± 1	NA	NA
miR-204 (212)	1	35 ± 5	0 ± 0	0 ± 0	0 ± 0	0 ± 1	NA	NA
miR-204 (250)	2	56 ± 5	0 ± 0	0 ± 0	0 ± 0	0 ± 1	NA	NA
miR-20 (210)	3	67 ± 5	0 ± 0	0 ± 0	0 ± 0	0 ± 1	NA	NA
miR-204 (3,120)	4	92 ± 5	0 ± 0	0 ± 0	0 ± 0	1 ± 3	92 ± 5	26 ± 3
miR-204 (167)	6	95 ± 5	0 ± 0	0 ± 0	0 ± 0	1 ± 3	NA	NA

n, number of injected embryos; NA, not analyzed.